

Repair of Critical-Sized Rat Calvarial Defects Using Genetically Engineered Bone Marrow-Derived Mesenchymal Stem Cells Overexpressing Hypoxia-Inducible Factor-1 α

DUOHONG ZOU,^{a,b,f} ZHIYUAN ZHANG,^b DONGXIA YE,^b AIFA TANG,^c LIANFU DENG,^d WEI HAN,^e JUN ZHAO,^b SHUHONG WANG,^a WENJIE ZHANG,^b CHAO ZHU,^b JIAN ZHOU,^f JIACAI HE,^f YUANYIN WANG,^f FENG XU,^b YUANLIANG HUANG,^g XINQUAN JIANG^b

^aSchool of Stomatology, Tongji University, Shanghai, China; ^bDepartment of Oral and Maxillofacial Surgery, Ninth People's Hospital Affiliated with Shanghai Jiao Tong University, School of Medicine, Shanghai Key Laboratory of Stomatology, Shanghai, China; ^cThe Second People's Hospital of Shenzhen, First Affiliated Hospital of Shenzhen University, China; ^dDepartment of Orthopaedics, Shanghai Institute of Orthopaedics and Traumatology, Shanghai Ruijin Hospital, Shanghai Jiaotong University School of Medicine, China; ^eDepartment of Oral and Maxillofacial Surgery, Nanjing Stomatological Hospital, Nanjing, China; ^fDepartment of Oral and Maxillofacial Surgery, School of Stomatology, Stomatological Hospital, Anhui Medical University, Hefei, China; ^gDepartment of Stomatology, Shanghai East Hospital Affiliated with Tongji University, Shanghai, China

Key Words. Hypoxia-inducible factor-1 α • Bone marrow-derived mesenchymal stem cells • Osteogenesis • Gene therapy • Bone regeneration

ABSTRACT

The processes of angiogenesis and bone formation are coupled both temporally and spatially during bone repair. Bone marrow-derived mesenchymal stem cells (BMSCs) have been effectively used to heal critical-size bone defects. Enhancing their ability to undergo angiogenic and osteogenic differentiation will enhance their potential use in bone regeneration. Hypoxia-inducible factor-1 α (HIF-1 α) has recently been identified as a major regulator of angiogenic-osteogenic coupling. In this study, we tested the hypothesis that HIF-1 α gene therapy could be used to promote the repair of critical-sized bone defects. Using lentivirus-

mediated delivery of wild-type (HIF) or constitutively active HIF-1 α (cHIF), we found that in cultured BMSCs *in vitro*, HIF and cHIF significantly enhanced osteogenic and angiogenic mRNA and protein expression when compared with the LacZ group. We found that HIF-1 α -overexpressing BMSCs dramatically improved the repair of critical-sized calvarial defects, including increased bone volume, bone mineral density, blood vessel number, and blood vessel area *in vivo*. These data confirm the essential role of HIF-1 α modified BMSCs in angiogenesis and osteogenesis *in vitro* and *in vivo*. *STEM CELLS* 2011;29:1380–1390

Disclosure of potential conflicts of interest is found at the end of this article.

INTRODUCTION

Repair of bone defects caused by severe trauma, resection of tumors, and congenital deformities remains a challenge for surgeons. Recently, tissue engineering has become a promising approach for bone regeneration. Successful repair of bone defects using this technique has been demonstrated using bone marrow-derived mesenchymal stem cells (BMSCs) as seed cells [1]. However, large numbers of functional seed cells are needed for the successful repair of a large bone

defect. Because of this requirement, genetically modified BMSCs with enhanced osteogenic and angiogenic activity will greatly broaden the application of BMSCs in tissue engineering for bone regeneration [2].

A previous study demonstrated that *hypoxia-inducible factor-1 α* (HIF-1 α) enhanced angiogenic and osteogenic gene expression and acted as a critical regulator of angiogenic-osteogenic coupling in a *HIF-1 α* knockout mice-model [3]. The HIF family comprises three α subunits: HIF-1 α , HIF-2 α , and HIF-3 α . HIF-2 α and HIF-3 α have limited homology with HIF-1 α , but all three subunits share a conserved von Hippel-

Author contributions: D.Z., Z.Z., D.Y., and A.T.: conception and design; L.D. and W.Z.: manuscript writing; W.H., J.Zhao, S.W., and C.Z.: performed research; J.Zhou and J.H.: collection and/or assembly of data; Y.W. and F.X.: provision of study material; Y.H. and X.J.: supervised the research and revised/approved the manuscript. D.Z., Z.Z., D.Y., and A.T. contributed equally to this article.

Correspondence: Yuanliang Huang, Ph.D. Department of Stomatology, Shanghai East Hospital Affiliated with Tongji University, 150 Jimo Road, Shanghai 200120, China. Telephone: 86-21-38804518; Fax: +86-21-58765119; e-mail: Yuanlianghuangyx@126.com; or Xinquan Jiang, Ph.D. Oral Bioengineering Lab/Regenerative Medicine Lab, Department of Prosthodontics, Shanghai Research Institute of Stomatology, Ninth People's Hospital, Shanghai Jiao Tong University School of Medicine, Shanghai Key Laboratory of Stomatology, Zhizhao Ju Road, Shanghai 200011, China. Telephone: 86-21-23271132; Fax: +86-21-63136856; e-mail: xinquanj@yahoo.cn Received February 23, 2011; accepted for publication July 2, 2011; first published online in *STEM CELLS EXPRESS* July 19, 2011. © AlphaMed Press 1066-5099/2009/\$30.00/0 doi: 10.1002/stem.693

Lindau protein (VHL)-binding domain and are consequently identically regulated by hypoxia [4]. In some cases, HIF-1 α and HIF-2 α can function redundantly to promote expression of downstream genes [5]. To the best of our knowledge, HIF-1 α is expressed in almost all cell types, while HIF-2 α is largely restricted to certain tissues such as blood vessels and the neural crest [6, 7]. Hundreds of genes have been identified as direct targets of HIF-1 α regulation, including vascular endothelial growth factor (VEGF) and stromal-derived factor 1 (SDF1) [8]. In normoxic states, prolyl hydroxylase is activated and hydroxylates proline residues 402 and 564 of HIF-1 α . HIF-1 α can then be bound by the VHL and substantially degraded. Hydroxylation of asparagine 803 by factor inhibiting HIF-1 can prevent binding to transcriptional coactivators CREB-binding protein (CBP) and p300 [9]. Hypoxia can inhibit the hydroxylation of both the asparagine and the prolines, which leads to a rapid increase in HIF-1 α [10]. Based on the above knowledge, Lenti-HIF (a lentivirus encoding wild-type HIF-1 α [HIF]) and Lenti-cHIF (a constitutively active form of mutated HIF-1 α [cHIF]) were constructed and used to test the function of HIF-1 α during osteogenesis and angiogenesis under normoxic conditions.

Tissue engineering combined with gene therapy represents a promising approach for bone regeneration [11]. BMSCs are multipotent stem cells that can be differentiated into bone, cartilage, fat, and other cell types [12]. Introduction of specific genes could dramatically tap into this osteogenic potential. In the past few decades, bone morphogenetic protein (BMP), runt-related transcription factor two (Runx2), and VEGF have been transduced into mesenchymal stem cells (MSCs), both separately and jointly, to increase the osteogenic and angiogenic activities of the cells [2, 13, 14]. Compared with the above genes, HIF-1 α has many advantages because it is an upstream gene involved in the transcriptional regulation of many genes with osteogenic and angiogenic effects. Thus, the application of BMSCs expressing a constitutively active form of HIF-1 α protein by adding an overexpressing HIF-1 α gene is a tempting approach for treatment. In this study, we explored whether HIF-1 α can induce BMSCs osteogenesis and angiogenesis, and using BMSCs overexpressing HIF-1 α to repair a critical-sized cranial defect in a rat model.

MATERIALS AND METHODS

Cell Culture and Gene Transduction

BMSCs were culture as previously described [15]. Total BMSCs were isolated from 4-week-old male Fisher 344 rats with a weight of 40 ± 5 g. Briefly, both ends of the femur were cut off at the epiphysis, and the marrow was flushed out using Dulbecco's modified Eagle's medium (DMEM) (Gibco BRL, Grand Island, NY, USA) containing 23 mM NaHCO₃ (Gibco Biocult, Paisley, U.K.) and supplemented with 10% heat-inactivated fetal bovine serum (FBS) (Gibco Biocult, Paisley, U.K.) and antibiotics (50 μ g/ml streptomycin sulfate and 100 U/ml penicillin). Cells were cultured in DMEM at 37°C in a humidified 5% CO₂ incubator. After three passages, cells were used for the experiments.

Total RNA was extracted from human BMSCs according to the protocol provided by the PrimeScript™ RT reagent Kit (TaKaRa Code: DRR037A). cDNAs were synthesized with Oligo dT primer using Reverse Transcription System Kit (Invitrogen, Carlsbad, CA, USA) following the manufacturer's instructions. HIF-1 α specific primers for cloning the full-

length open reading frame of HIF-1 α (2481 bp) were designed using Oligo software based on human HIF-1 α mRNA sequences from GenBank (NM_001530). The amplified cDNA was first constructed into the vector of IRES2-enhanced green fluorescent protein (EGFP) (BD #6029-1) and further subcloned into FUGW backbone vector as described previously [16]. Virus particles were packaged by transfection of 293T cell line with the above cloned flap-Ub promoter-GFP-WRE (FUGW) and other two packaging plasmids Pax-2 and Vsvg. After 48 hours of post-transfection, the virus particles in culturing medium were collected and titered by infection of 293T cell with series diluent of the original culturing medium. A multiplicity of infection of 15 was used to infect the BMSCs, the infection efficiency was detected by fluorescence microscopy analysis of green fluorescent protein and approximately 90% efficiency were observed. The protocol concerning to the use of human cells was approved by the Independent Ethics Committee of Shanghai Ninth Peoples' affiliated to Shanghai JiaoTong University, School of Medicine.

Lenti-HIF-1 α is a replication-defective lentivirus that encodes EGFP and human HIF-1 α . According to data described previously [9], HIF-1 α was mutated in this study to effectively maintain the stability and activity of HIF-1 α under normoxia conditions. Lenti-cHIF has the following mutations: proline 564 to alanine, proline 402 to alanine, and aminosuccinic acid 803 to alanine (Supporting Information Fig. S1). The mutageneses were confirmed by DNA sequencing analysis. After gene transduction, an HIF-1 α antibody (red) and 4,6-diamino-2-phenyl indole (DAPI) (blue) were used to locate the protein expression in the cells by immunofluorescence. Cell viability was determined by the dimethylthiazol-2-yl-2, 5-diphenyl-tetrazoliumbromide (MTT). As reported previously [17], BMSCs were seeded onto the 96-well plates at a density of 5,000 cells per 100 microlitre per well. After 1–7 days of culture, the cell proliferation was evaluated by 3-(4,5-dimethylthiazol-2-yl)-5-(3-carboxymethoxyphenyl)-2-(4-sulfo-phenyl)-2H-tetrazolium (MTS) assay (Promega Corp., Madison, WI, USA). A 20- μ l of MTS solution was added and cells were incubated at 37°C for 4 hours. Absorbance at 490 nm was measured using a microplate reader. For cell proliferation assay, BMSCs transduced with Lenti-HIF, Lenti-cHIF, and Lenti-LacZ were seeded at a density of 2×10^5 cells per well in a six-well plate containing 10% FBS-DMEM. The cells were harvested with 0.05% trypsin and 0.5 mM EDTA. The total number of cells was counted using the Z2 Coulter Counter (Beckman Coulter Inc., CA, USA). The cell count was determined on days 0, 1, 4, and 7. The assay was repeated three times.

ALP Activity and ARS Staining

BMSCs transduced with Lenti-HIF, Lenti-cHIF, and Lenti-LacZ were plated on six-well plates at a density of 10^5 cells per well and cultured in DMEM at 37°C in a humidified 5% CO₂ incubator. They were then evaluated for alkaline phosphatase (ALP) and deposit of mineralization (alizarin red staining [ARS]) on days 14 and 21 after transduction. Semi-quantitative analysis of ALP and alizarin red S (ARS) was performed following a standard protocol [18]. To measure ALP, cells were rinsed three times with phosphate-buffered saline (PBS) and lysed with Triton X-100. The total protein content of aliquots of these samples was determined using the bicinchoninic acid (BCA) method with a Pierce (Rockford, III) protein assay kit. ALP activity was determined at 405 nm using *p*-nitrophenyl phosphate (Sigma-Aldrich, St. Louis, MO, USA) as the substrate. To prepare the cells for calcium nodule measurements, cells were washed three times in PBS and

Table 1. Nucleotide sequences for real-time polymerase chain reaction primers

Genes	Primer sequence (5'-3') (forward/reverse)	Product size (bp)	Annealing temperature (°C)	Accession number
<i>HIF-1α</i>	CCCTACTATGTCGCTTTCTTGG GTTTCTGCTGCCTTGATGGG	199	60	NM_001530.3
<i>VEGF</i>	GGCTCTGAAACCATGAACTTCT GCAATAGCTGCGCTGGTAGAC	165	60	NM_031836.2
<i>SDF1</i>	ACCTCGGTGTCCTCTTGCTG GATGTTTGACGTTGGCTCTGG	164	60	NM_001033883.1
<i>OCN</i>	CAGTAAGGTGGTGAATAGACTCCG GGTGCCATAGATGCGCTTG	172	60	NM_013414.1
<i>BMP-2</i>	AGCAGCCTCAACTCAAACCTCG CGTCAGAGGGCTGGGATG	158	60	NM_017178.1
<i>BSP</i>	TGGATGAACCAAGCGTGGA TCGCCTGACTGTCGATAGCA	162	60	NM_012881.2
<i>ALP</i>	GTCCACAAAGAGCCACAAT CAACGGCAGAGCCAGGAAT	172	60	NM_013059.1
<i>Runx2</i>	TCTTCCCAAAGCCAGAGCG TGCCATTTCGAGGTGGTCG	154	60	NM_053470.1
<i>OPN</i>	TGGATGAACCAAGCGTGGA TCGCCTGACTGTCGATAGCA	168	60	NM_012881.2
<i>GAPDH</i>	GGCAAGTTCAACGGCACAGT GCCAGTAGACTCCACGACAT	76	60	NM_017008.3

fixed in cold 70% ethanol for 1 hour. The cells were then stained with ARS (40 mM) for 20 minutes at room temperature. The stain was desorbed with 10% cetylpyridinium chloride (Sigma-Aldrich, St. Louis, MO, USA) for 1 hour. The solution was collected and distributed at 100 μ l per well on 96-well plate for absorbance reading at 590 nm with a spectrophotometer (Thermo Spectronic, California, USA). Finally, ALP and ARS levels were normalized to the total protein content. All experiments were conducted in triplicate.

qRT-PCR and Western Blotting Analysis

Total cellular RNA extraction was performed with an RNeasy Mini kit (Qiagen, Hilden, Germany) on days 0, 1, 4, 7, 14, and 21 after gene transduction. The quality and quantity of RNA were checked by spectrophotometric analysis using a biophotometer (Eppendorf BioPhotometer Plus, Eppendorf, Germany). Reverse transcription was carried out using 1 μ g of total RNA in a final volume of 20 μ l using a PrimeScript RT reagent kit (Takara Bio, Shiga, Japan) according to the manufacturer's recommendations. The real-time polymerase chain reaction (RT-PCR) was performed with an instrument named MX3000 from Stratagene, and the relative expression of each target mRNA was calculated using the comparative ΔC_t method as the reference [19]. Gene-specific primers were synthesized commercially (Shengong Co., Ltd. Shanghai, China), and the genes, accession numbers, primer sequences, and amplicon sizes are listed in Table 1. All mRNA values were normalized against glyceraldehyde 3-phosphate dehydrogenase (GAPDH) expression.

Total protein was harvested from cultured cells on days 0, 1, 4, 7, 14, or 21 after gene transduction. The procedure was performed according to standard protocols. Cells were washed twice with PBS and incubated in 200 μ l lysis buffer (20 mM Tris-Cl, 150 mM NaCl, 1% Triton X-100, 1 mM EDTA, 2 mM sodium orthovanadate, 50 mM sodium fluoride, 2 μ g/ml pepstatin A, 10 μ g/ml aprotinin, and 10 μ g/ml leupeptin) on ice for 30 minutes with occasional agitation. Protein concentrations were measured using the DC protein assay kit (Invitrogen, Carlsbad, CA). Equal amounts of cell lysates were separated on duplicate 8%–10% SDS-polyacrylamide

gel electrophoresis (PAGE) gels and transferred to a polyvinylidene difluoride membrane (0.45 μ m, Millipore, Bedford, MA, USA). Membranes were incubated with specific primary antibodies overnight at 4°C at a 1:600 dilution. Membranes were then washed three times with Tris-HCl-buffered saline (TBS) containing 0.1% Tween 20 detergent and incubated for 2 hours with horseradish-peroxidase (HRP)-conjugated secondary antibodies. ECL Plus Western blotting detection reagent (GE Healthcare Bio-Sciences, Uppsala, Sweden) was used to detect immunoreactive products. Protein bands were visualized using the Enhanced Chemiluminescence system (Amersham Pharmacia Biotech Inc., USA) and Kodak X-OMAT film (Rochester, New York). The same procedure was used for antibodies against other proteins, including VEGF, SDF1, BMP-2, Runx2, osteocalcin (OCN), osteopontin (OPN), and bone sialoprotein (BSP) (Abcam, Inc., AC, U.K.). Relative protein levels were normalized against β -actin. All experiments were performed in triplicate. Results are reported as the mean \pm SD.

Animal Experiments

All procedures were approved by the Tongji University Committee on the Use and Care of Animals and were in compliance with state laws. Four days after BMSCs transduced with Lenti-LacZ, Lenti-HIF, and Lenti-cHIF, cells were trypsinized and seeded on a gelatin sponge (GS) (Gelfoam; Upjohn, Kalamazoo, MI, U.S.A.). Two million cells were used in each implant (3 \times 5 \times 5 mm³) for a total of 12 implants with six rats per group (Supporting Information Fig. S2A–S2D and [20]). Besides, GS was used as negative control for critical-sized defects repair. Surgical procedures were performed on 12-week-old male Fisher 344 rats as described previously [21]. Briefly, the animals were anesthetized by intraperitoneal injection of pentobarbital (Nembutal 3.5 mg/100 g). A 1.0- to 1.5-cm sagittal incision was made on the scalp, and the calvarium was exposed by blunt dissection. Two critical-sized defects were created by means of a 5-mm diameter trephine burr (Fine Science Tools, Foster City, CA, USA). Preformed GS seeded with Lenti-LacZ-, Lenti-HIF- or Lenti-MT-treated BMSCs were placed in the defects, and the incision was

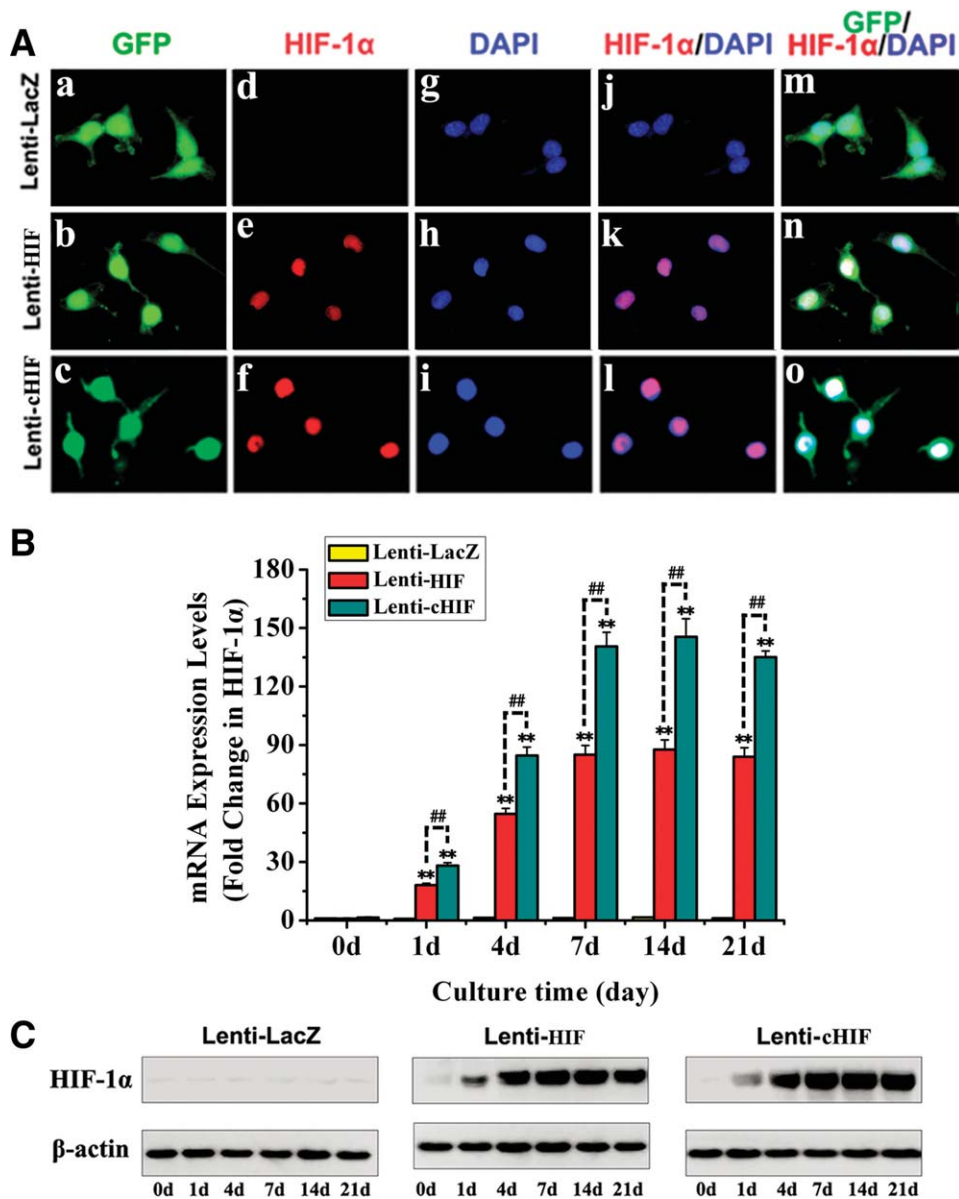


Figure 1. Detection of HIF-1 α after gene transduction. Immunofluorescence detection (A); hypoxia-inducible factor-1 α (HIF-1 α) mRNA expression in HIF, constitutively active HIF-1 α (cHIF), and LacZ groups on days 0, 1, 4, 7, 14, and 21 (B); Protein expression levels in the bone marrow-derived mesenchymal stem cells transduced by Lenti-HIF, Lenti-cHIF, and Lenti-LacZ (C). ##, ##, $p < .01$ (the cHIF group comparing with the HIF group); **, **, $p < .01$ (target gene groups comparing with the LacZ group). Abbreviations: cHIF, constitutively active HIF-1 α ; DAPI, 4,6-diamino-2-phenyl indole; GFP, green fluorescent protein; HIF-1 α , hypoxia-inducible factor-1 α

closed in layers using 4-0 resorbable sutures. Cranial bones were harvested 8 weeks after implantation. All cranial samples were perfused with Microfil (Flowtech, Carver, MA, USA) after euthanasia to evaluate blood vessel formation as previously described [22]. After the animals were sacrificed, an incision was made from the abdomen to the chest. The descending aorta was found, and an angiocatheter was used to penetrate it. Next, the angiocatheter was fixed in the descending aorta using 4-0 sutures. The vena cava was incised, and perfusion of 20 ml of physiological saline was started immediately (100 U/ml at 2 ml/minutes using a syringe). A solution of Microfil was prepared in a volume ratio of 4:5 of Microfil: diluent with 5% curing agent. Following perfusion with saline, 20 ml of the Microfil solution was perfused at 2 ml/minutes.

Radiography and Micro-CT Measurement

The specimens were harvested at 8 weeks postoperatively, and bone volume (BV) in the skull was assessed using a desktop microtomographic imaging system (MicroCT-80, Scanco Medical, Bassersdorf, Switzerland) as reported previously [23]. Briefly, the specimens were scanned with an x-ray tube potential of 80 kV, a tube current of 0.45 mA and 15 μ m voxel resolution. A total scan time was 15 minutes and an estimated entrance dose of 30 cGy. Three-dimensional isosurface renderings were made for the visualization of bone with software. To obtain parameters of BV fraction and bone mineral densities (BMDs) in the defect areas, the gray-values of the voxels were stratified in a histogram running from 225 to 500 with a range of 25. Micro-CT measurements included BV

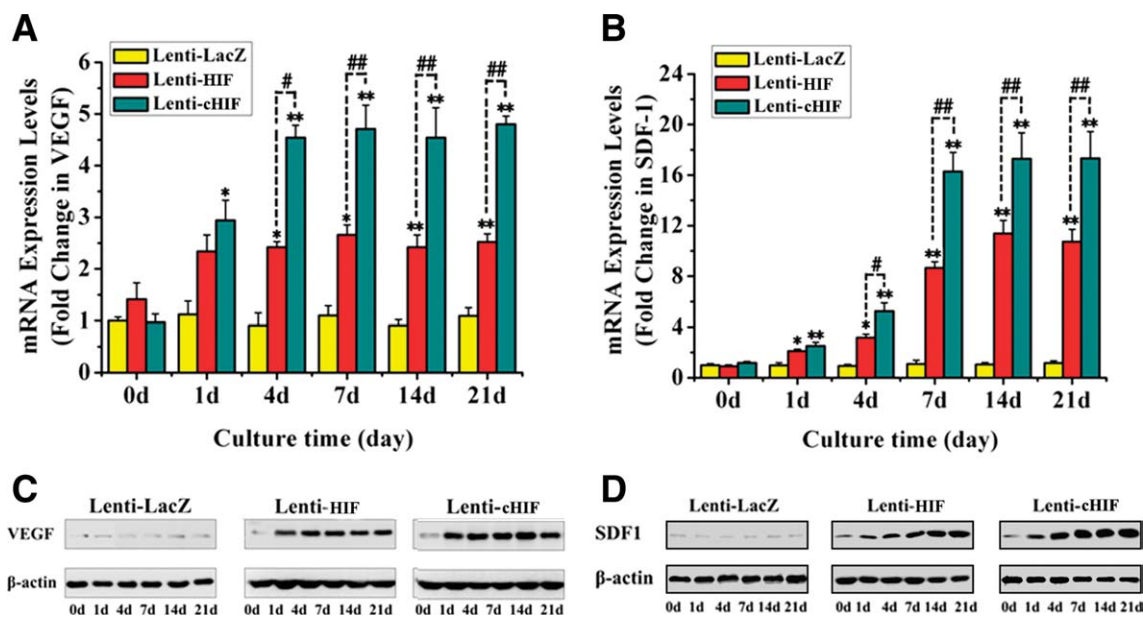


Figure 2. mRNA and protein expression of angiogenic factors was examined. mRNA expression of vascular endothelial growth factor (VEGF) and stromal-derived factor 1 (SDF1) (A, B). Protein expression of VEGF and SDF1 (C, D). *, $p < .05$ and **, $p < .01$ (target gene groups comparing with the LacZ group), #, $p < .05$ and ##, $p < .01$ (the constitutively active hypoxia-inducible factor (HIF)-1 α group comparing with the HIF group). Abbreviations: cHIF, constitutively active HIF-1 α ; HIF, hypoxia-inducible factor; SDF1, stromal-derived factor 1; VEGF, vascular endothelial growth factor.

to total bone volume (BV/TV) and local BMDs in the bone defect. X-ray images of skulls were taken with the imaging system FX Pro (Kodak, America).

Histological and Histomorphometric Observation

Skulls were harvested and fixed in a 5% neutral buffered formalin solution. The specimens were dehydrated in ascending concentrations of alcohol from 75% to 100% and then embedded in polymethylmethacrylate. The undecalcified specimens were cut in 150- μ m-thick sections obtained by means of a microtome (Leica, Hamburg, Germany). The orientation of the sections was selected on sagittal surface in each animal. Three sections, representing the central area of each defect were used for the histometric analysis, and then the sections were polished to a final thickness of approximately 40 μ m as described previously [24]. Then, the sections were stained with van Gieson's picro fuchsin for histologic observation. Areas of newly formed bone were quantified using Image Pro 5.0 (Media Cybernetics, USA) and reported as a percentage among whole bone defect area. The reproducibility of the method of measurement was conducted in triplicate. No statistically significant differences were found between the three recordings for any of the measured parameters. The number of blood vessels (blue spots by Microfil perfusion) in the specimens also was measured as number and areas among whole bone defect area.

Statistical Analysis

Results are presented as mean \pm SD. Statistical significance was assessed by analysis of variance (ANOVA) with a Tukey's post hoc test. $p < .05$ was considered statistically significant. (*, $p < .05$ and **, $p < .01$, target gene groups comparing with the control group; #, $p < .05$ and ##, $p < .01$, the cHIF group comparing with the HIF group).

RESULTS

Immunofluorescence, MTT, and Cell Proliferation

Overexpression of HIF-1 α was detected in the Lenti-HIF, Lenti-cHIF, and Lenti-LacZ groups by immunofluorescence. HIF-1 α expression was significantly enhanced in the Lenti-HIF- and Lenti-cHIF-transduced groups when compared with Lenti-LacZ (control) group which was barely detectable. Red fluorescence of the HIF-1 α protein overlapped with blue nucleolus, demonstrating its expression location in BMSCs (Fig. 1A). To investigate the effect of HIF-1 α on BMSCs growth, MTT assay and cell count was carried out after treating cells with Lenti-LacZ, the Lenti-HIF and Lenti-cHIF for 0–7 days. We found that target gene could increase BMSCs proliferation comparing with LacZ group (Supporting Information Fig. S3A, S3B).

qRT-PCR and Western Blotting Analysis of HIF-1 α -Induced Osteogenesis and Angiogenesis Expression In Vitro

To examine the expression levels of angiogenic and osteogenic markers in HIF-1 α -overexpressing BMSCs, quantitative RT-PCR (qRT-PCR) and western blotting was performed on days 0, 1, 4, 7, 14, and 21. HIF-1 α was clearly overexpressed in the Lenti-HIF and Lenti-cHIF groups when compared with the LacZ group (Fig. 1B, 1C). VEGF and SDF1, important angiogenic factors, were initially upregulated on day 4 in the Lenti-HIF and Lenti-cHIF groups, and a notable increase was observed from days 7 to 21. At the same time, mRNA expression from the cHIF group was one- to twofold higher than the HIF group on days 7 to 21 (Fig. 2A, 2B). Protein results showed that expression of VEGF and SDF1 increased by two- to fourfold in the Lenti-HIF and Lenti-cHIF groups in comparison with the Lenti-LacZ group from days 4 to 21 (Fig. 2C, 2D). This finding suggests that HIF-1 α -overexpressing BMSCs may have enhanced angiogenic properties. The

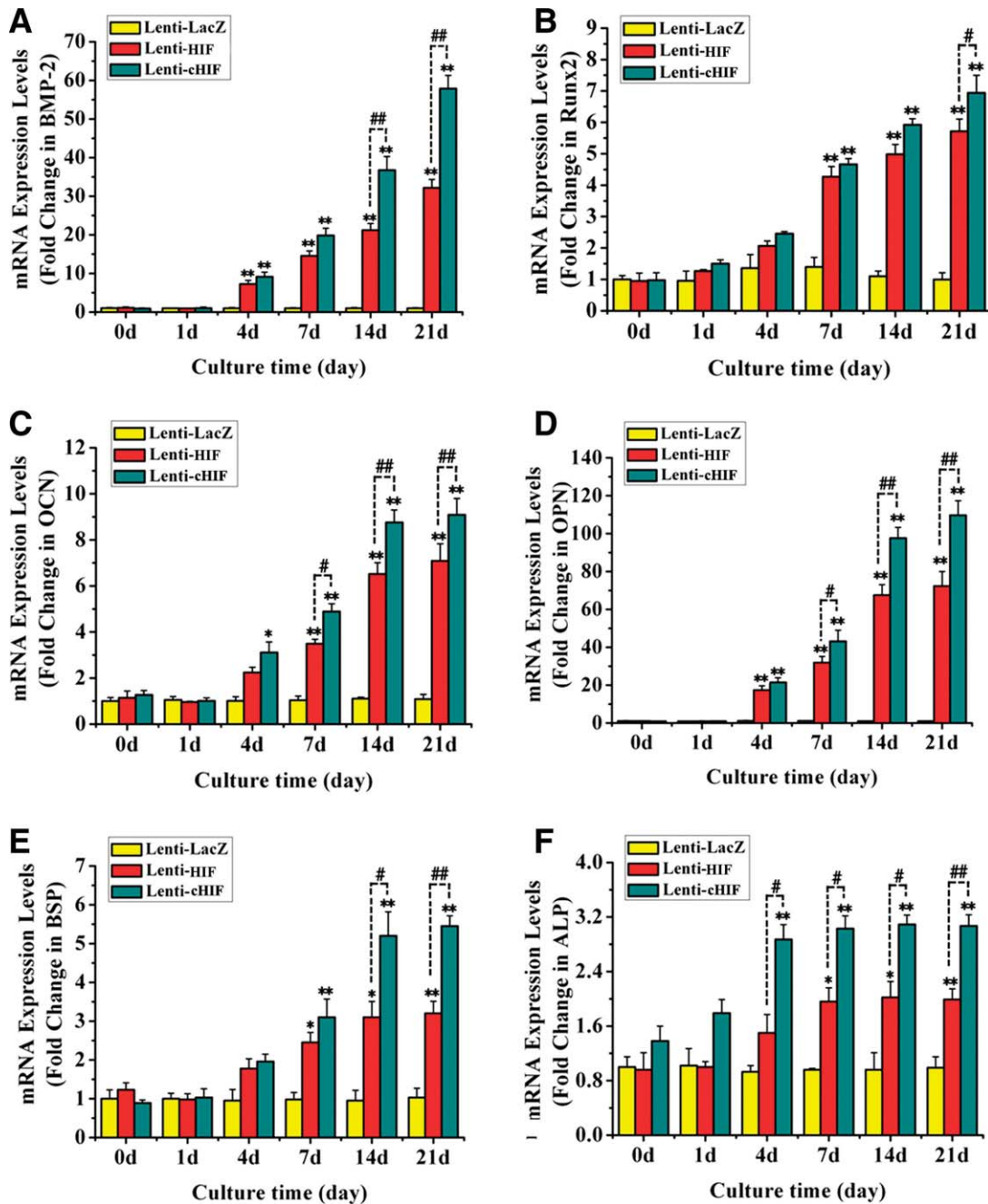


Figure 3. Detection of mRNA and protein expression of osteogenic markers. mRNA expression of bone morphogenetic protein 2 (A), Runx2 (B), osteocalcin (C), osteopontin (D), bone sialoprotein (E), and alkaline phosphatase (F); protein expression of these osteogenic factors (G). *, $p < .05$ and **, $p < .01$ (target gene groups comparing with the LacZ group or GS group), #, $p < .05$ and ##, $p < .01$ (the cHIF group comparing with the HIF group). Abbreviations: ALP, alkaline phosphatase; BMP-2, bone morphogenetic protein 2; BSP, bone sialoprotein; cHIF, constitutively active HIF-1 α ; HIF, hypoxia-inducible factor; OCN, osteocalcin; OPN, osteopontin.

mRNA expression of BMP-2 increased markedly on day 4 and then increased continuously from days 7 to 21. For example, on day 21, BMP-2 mRNA expression was increased 57 folds in the cHIF group and 32 folds in the HIF group, but only threefolds in the LacZ group compared with those on day 0 (Fig. 3A). Protein expression of BMP-2 was increased eight- to ninefold in the Lenti-HIF and Lenti-cHIF groups in comparison with the Lenti-LacZ group on day 21 (Fig. 3G). However, the expression of Runx2 mRNA initially increased on day 7 and then increased continuously from days 14 to 21(Fig. 3B). The protein expression was the same tendency as

mRNA levels (Fig. 3G). Other pivotal osteogenic genes or proteins such as ALP, BSP, OCN, and OPN demonstrated similar tendencies as BMP-2 or Runx2 (Fig. 3C–3G). Overall, transcripts of osteogenic markers in the LacZ group remained at low levels. However, Lenti-cHIF was more effective at inducing expression of angiogenesis and osteogenesis markers in BMSCs in vitro than Lenti-HIF. This tendency may attribute to cHIF with its higher resistance to degradation so as to maintain its activity under normoxia. Taken together, these data support the hypothesis that osteoinductive and angiogenic effects in BMSCs can be enhanced by overexpress of HIF-1 α .

ALP and ARS

On days 14 and 21 after gene transduction, ALP expression was significantly enhanced in the Lenti-HIF and Lenti-cHIF

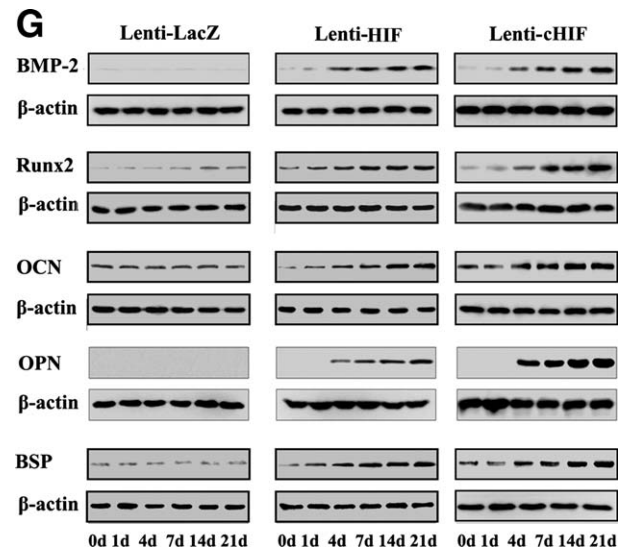


Figure 3. Continued

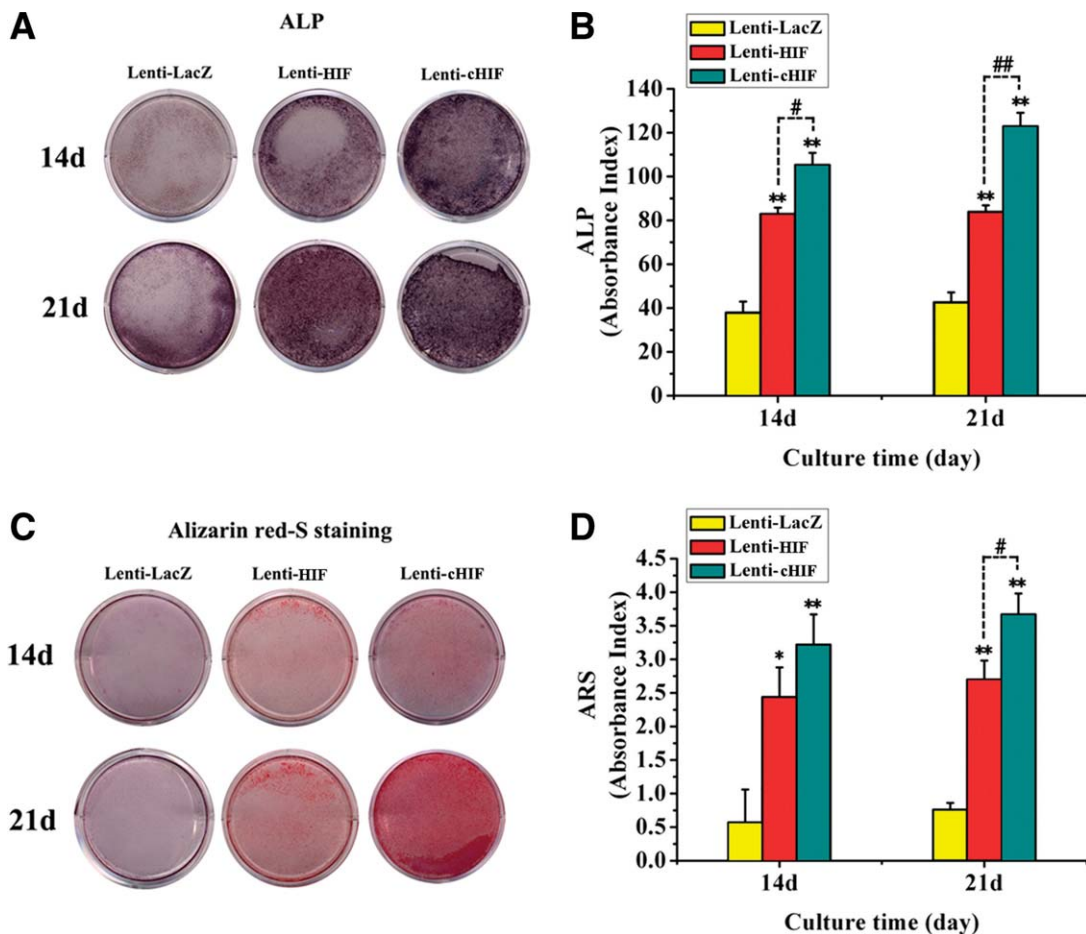


Figure 4. Analysis of alkaline phosphatase (ALP) staining and alizarin red staining (ARS). ALP expression on days 14 and 21 (A); semiquantitative analysis of ALP activity (B); the results of ARS staining (C); and semiquantitative analysis of ARS (D). Abbreviations: BMP-2, bone morphogenetic protein 2; BSP, bone sialoprotein; cHIF, constitutively active HIF-1 α ; HIF, hypoxia-inducible factor; OCN, osteocalcin; OPN, osteopontin. *, $p < .05$ and **, $p < .01$ (target gene groups comparing with the LacZ group or GS group), #, $p < .05$ and ##, $p < .01$ (the cHIF group comparing with the HIF group).

groups (Fig. 4A). Furthermore, ARS staining on day 21 revealed significant increases in calcium deposition in the Lenti-HIF and Lenti-cHIF groups (Fig. 4C). The semiquantitative analysis showed that ALP activity in Lenti-HIF and Lenti-cHIF groups was two- to threefold higher than the control group on days 14 and 21 (Fig. 4B). In addition, semiquantitative analysis of the ARS results showed that the absorbance index values from the HIF-1 α gene transduced groups were four- to fivefold higher than the control group on days 14 and 21 (Fig. 4D). These results are consistent with the gene and protein expression of osteogenic markers in BMSCs overexpressing HIF-1 α in vitro. All of these results show that HIF-1 α promotes osteogenic activity in BMSCs.

HIF-1 α Gene Improving Healing of Critical-Sized Rat Calvarial Defects In Vivo

To evaluate newly formed bones in rat model, radiographic examination was performed 8 weeks after the implantation of BMSCs in defect areas. A large, defined radio-opaque mass representing new bone formation and mineralization was observed in both Lenti-HIF- and Lenti-cHIF-transduced BMSCs groups (Fig. 5A). Compared with the Lenti-LacZ group and the GS group, the radiopacity of the target gene (HIF and cHIF) groups was close to that of the normal skull structure. Morphology of the newly formed bone was also detected by micro-CT. Substantial formation of plate-like

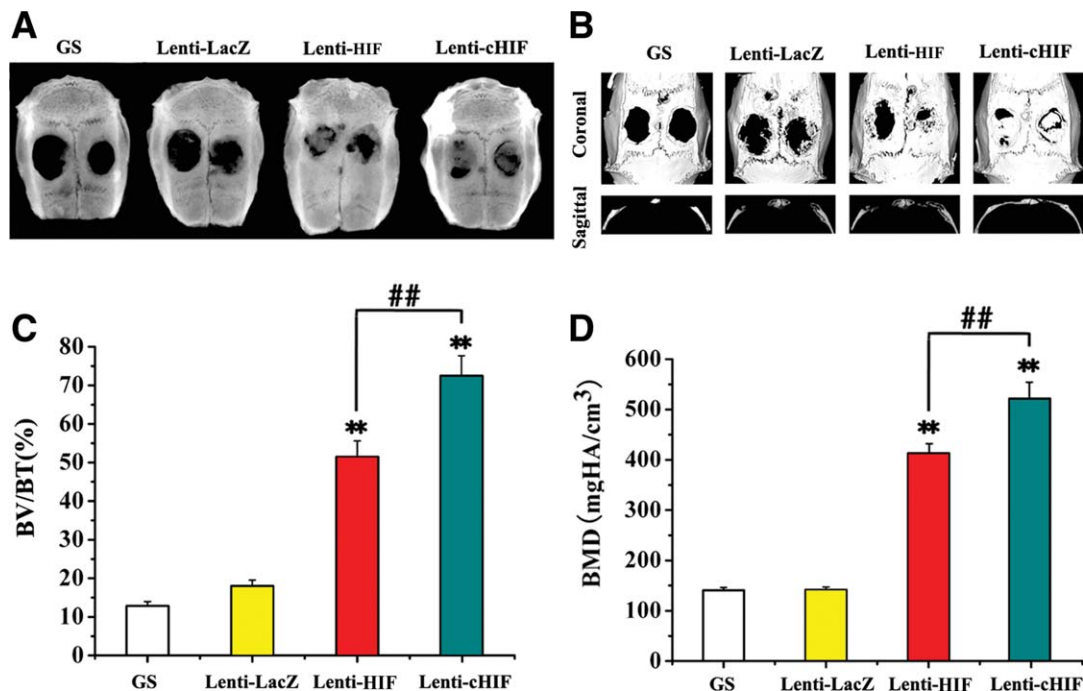


Figure 5. Radiography and micro-CT evaluation of the repaired skull at 8 weeks after implantation. Gelatin sponge (GS) constructs, Lenti-LacZ-transduced bone marrow-derived mesenchymal stem cells (BMSCs)/GS constructs, Lenti-hypoxia-inducible factor (HIF)-transduced BMSCs/GS constructs, and Lenti-constitutively active HIF-1 α (cHIF)-transduced BMSCs/GS constructs (from left to right). Representative photographs showed large defined radiopacities at the defect sites (A). Micro-CT images of calvarial defects taken 8 weeks after implantation (B). Morphometric analysis of new bone formation (C) and local bone mineral density (D). *, $p < .05$ and **, $p < .01$ (target gene groups comparing with the LacZ group or GS group), #, $p < .05$ and ##, $p < .01$ (the cHIF group comparing with the HIF group). Abbreviations: ALP, alkaline phosphatase; ARS, alizarin red staining; cHIF, constitutively active HIF-1 α ; HIF, hypoxia-inducible factor.

bone structures was visible in the center of the defect site 8 weeks after treatment with target gene-transduced BMSCs. The new bone had expanded and occupied almost the whole region of the bone defect observed by coronal and sagittal surface (Fig. 5B). Quantitative analysis of the newly formed bone was performed using morphometrical methods. This analysis confirmed that more bone formation occurred in the target gene groups (**, $p < .01$). The ratio of new BV to total BV (BV/TV, %), which indicates the relative amount of newly formed bone, was 72.58% in the cHIF group, 55.75% in the HIF group, 17.59% in the LacZ group, and 14.82% in the GS group (Fig. 5C). Local BMDs demonstrated the same tendencies that bone formation was more in the target gene groups than the control group (Fig. 5D). Under light microscopy, the undecalcified specimens in the Lenti-HIF and Lenti-cHIF groups demonstrated a significant amount of new bone formation, even at the center portion of the implant. Histological findings further supported the radiographic data (Fig. 6A). To assess vascularization, Microfil perfusion was performed and the number of blood vessels was 10 ± 1 blood vessels per $100\times$ field in the Lenti-HIF group, 13 ± 1 per square micrometre in the Lenti-cHIF group, 4 ± 1 per square micrometre in the Lenti-LacZ group, and 3 ± 1 per square micrometre in the GS group (Fig. 6B). The results of vessel luminal area were conformity with the number of blood in sections (Fig. 6C). The increased vessel number and luminal area provided a histological foundation for increased blood flow and improved the environment for bone formation. To evaluate ossification, sections were stained with van Gieson's picro fuchsin. The newly formed bone area was $0.54\% \pm 0.02\%$ of total area per $100\times$ field in the cHIF group, $0.42\% \pm 0.01\%$ of total area per $100\times$ field in the HIF group, $0.15\% \pm 0.01\%$ of total area per $100\times$ field in the LacZ

group, and $0.02\% \pm 0.01\%$ of total area per $100\times$ field in the GS (Fig. 6D).

DISCUSSION

This study investigated a therapeutic strategy based on HIF-1 α -transduced BMSCs for healing a critical-sized cranial defect. Our results indicate that overexpression of HIF-1 α may be a useful method to enhance BMSCs-mediated osteogenesis and angiogenesis.

A number of studies have demonstrated that the HIF-1 α protein is subject to ubiquitination and proteasomal degradation under nonhypoxic conditions [25]. To effectively maintain stability and activity in a normoxic state, cHIF was constructed. Mutating proline 564 to alanine and proline 402 to alanine stabilized HIF-1 α by preventing it from combining with VHL and being degraded. Mutating aspartic acid 803 to alanine enhanced HIF-1 α binding to the transcriptional coactivators CBP and p300 in normoxic conditions. Expression of HIF-1 α mRNA and protein in BMSCs transduced with Lenti-cHIF was greater than in HIF or LacZ groups in vitro. These results confirmed that the stability and activity of HIF-1 α could be effectively maintained in normoxic conditions by method of Lenti-cHIF transduction.

The expression levels of virtually all critical angiogenic growth factors are regulated by HIF-1 under hypoxia condition [26, 27]. To observe the expression of angiogenic marker genes in HIF-1 α gene-transduced BMSCs in vitro, VEGF and SDF1 were investigated at both the mRNA and protein levels. These two factors were upregulated in the target gene-treated BMSCs groups on day 4 and demonstrated a sustained

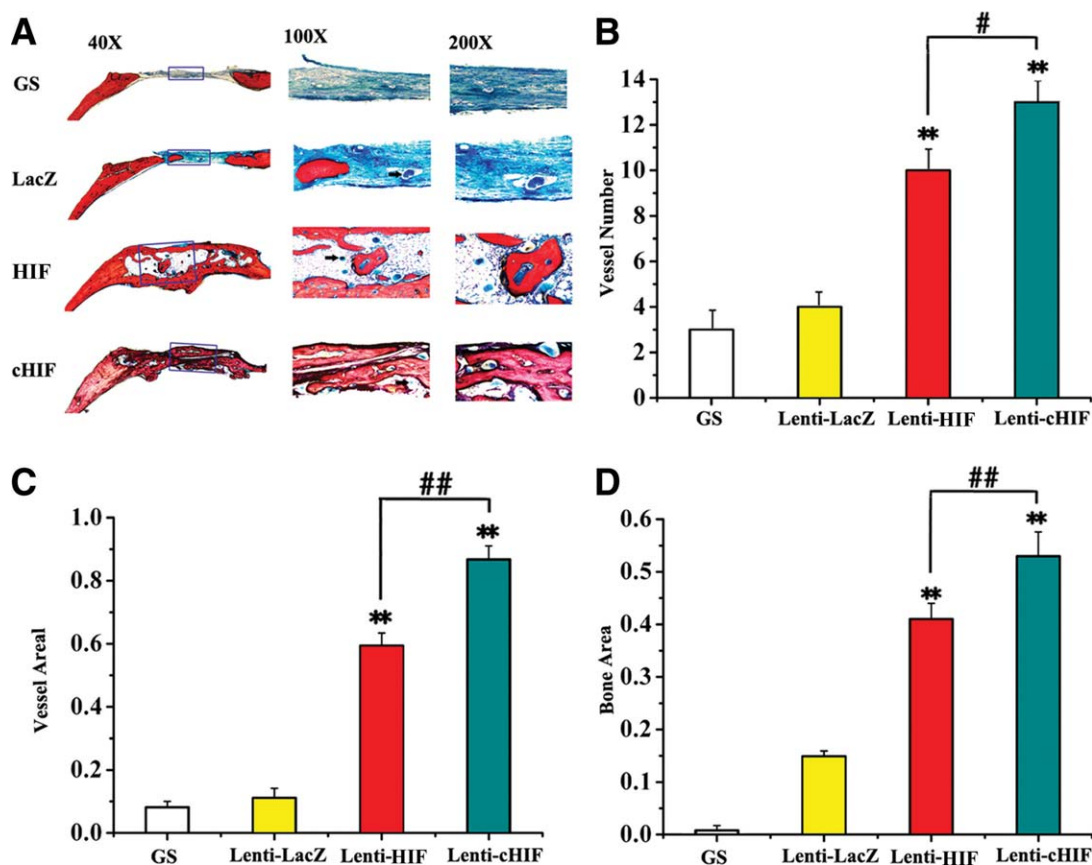


Figure 6. Histological analysis of newly formed bone and blood vessels in calvarial defects. After the Microfil stain used, the specimens were sliced and sections were stained with van Gieson's picro fuchsin. From top to bottom: gelatin sponge (GS) constructs, Lenti-LacZ-transduced bone marrow-derived mesenchymal stem cells (BMSCs)/GS constructs, Lenti-hypoxia-inducible factor-transduced BMSCs/GS constructs, and Lenti-constitutively active hypoxia-inducible factor-1 α -transduced BMSCs/GS constructs (original magnification, 40 \times , 100 \times , 200 \times , black arrows indicate blood vessels) (A). Mean number and area of blood vessels per 100 \times field in new bone sections (B, C). New bone formation area per 100 \times field in sections (D). **, $p < .01$ (target gene groups comparing with the LacZ group or GS group), ##, $p < .01$ (the cHIF group comparing with the HIF group). Abbreviations: BMD, bone mineral density; VT, total bone volume; BV, bone volume; cHIF, constitutively active HIF-1 α ; GS, gelatin sponge; HIF, hypoxia-inducible factor.

increase from days 7 to 21. This finding proved that *HIF-1 α* could enhance angiogenic activities of BMSCs in vitro and demonstrated the possibility of using HIF-1 α -overexpressing BMSCs to induce enhanced angiogenesis in the area of the bone defect in vivo.

Previous reports based on gene knockout technology have suggested that *HIF-1 α* might play important roles for bone formation [2]. However, there have been no reports on bone repair by using *HIF-1 α* gene therapy in animal models. As an upstream gene of VEGF and SDF1, *HIF-1 α* is hypothesized to have the ability to induce increased expression of osteogenic and angiogenic marker genes. However, to our knowledge, there are no reports on whether *HIF-1 α* can induce osteogenesis and angiogenesis in BMSCs in vitro and in vivo. To prove our hypothesis, mRNA expression levels of six key osteogenic factors, specifically BMP-2, Runx2, ALP, OCN, OPN, and BSP were detected in gene-modified BMSCs. These factors were all upregulated in both Lenti-HIF and Lenti-cHIF groups on day 4. Among these genes, the expression of BMP-2 showed greatest response with 30- to 50-fold increases on day 21. BMPs are a family of growth factors that have demonstrated an impressive ability to induce orthotopic and ectopic new bone formation [28]. BMPs are pleiotropic signaling molecules critically involved at various stages in bone formation. Among the

BMPs, BMP-2 has the strongest and most significant biologic activities [29]. Besides the qRT-PCR analysis, we also investigated the protein expression of above osteogenic genes. The protein levels were in good accordance with the mRNA levels. Furthermore, ALP and ARS analysis confirmed the osteoblastic differentiation of *HIF-1 α* -overexpressing BMSCs in vitro. These findings further convinced us that *HIF-1 α* -overexpressing BMSCs promoted osteogenic differentiation and might be used to repair bone defects in vivo. Additionally, expression of mRNA and protein in the cHIF group was greater than in the HIF and LacZ groups, which means that the stability and activity of HIF-1 α was best preserved in the cHIF group.

Interestingly, the MTT assay and cell count analysis showed that BMSCs proliferation in Lenti-cHIF and Lenti-HIF groups was increased obviously compared with LacZ group. Underlying mechanism remains unknown. However, it has been shown that the number of MSCs is increased in an oxygen-reduced environment [30]. Hypoxia can help to increase HIF-1 expression. Therefore, *HIF-1 α* may be responsible for the proliferation of MSCs under hypoxic conditions.

To explore the potential clinical applications of *HIF-1 α* , an in vivo study on the ability of *HIF-1 α* -modified BMSCs to repair a critical-sized cranial defect was performed. Due to

the advantages in flexibility, biocompatibility, biodegradability, and radiotransparency, GS have been regarded as a promising scaffold for bone regeneration [31]. In this study, GS were used as a biomaterial scaffold for *HIF-1 α* -modified BMSCs to keep cells suspended during implantation and regeneration. Radiological evaluation revealed that HIF- and cHIF-transduced cells almost repaired the whole defect area at week 8. More intensive bone formation was detected in the cHIF group than in the HIF group, whereas only minor repairs were observed in the LacZ and GS groups. Histological examination of the cHIF group bones demonstrated that the newly formed bone almost covered the entire area of the bone defect. Consistent with the above findings, quantitative analysis by micro-CT with the data acquired from both BMD and BV/TV revealed that there was much more newly formed bone in the cHIF group than in the HIF, LacZ, and GS groups (###, $p < .01$, **, $p < .01$). Interestingly, based on the histological examination, the blood vessel density was in good agreement with the bone area in calvarial defects. These results indicated that *HIF-1 α* was a major regulator of angiogenic-osteogenic coupling in bone formation. And support the idea that *HIF-1 α* gene could significantly improve ossification and vascularization in calvarial models.

Recently, other groups have reported increased vessel density and luminal area in ischemic limbs after intramuscular injection of *HIF-1 α* vectors [32]. Their studies are really encouraging for the potential clinical use of *HIF-1 α* in reconstructing blood vessels. However, to our knowledge, there are no previous reports on bone repair with *HIF-1 α* gene therapy. This might be partly due to the difficulty of effectively repairing critical-sized bone defects by injecting HIF-1 α vectors. Our study shows that using genetically engineered BMSCs can greatly improve the repair of critical-sized rat calvarial defects. Our findings proved that HIF-1 α can enhance BMSCs-induced angiogenic activity and osteogenesis both in vitro and in vivo. Temporally and spatially, the processes of angiogenesis and osteogenesis are coupled during skeletal regeneration. Blood vessels not only transport oxygen and nutrients but also play an important role in bone formation and remodeling by mediating the interaction between osteoblasts, osteocytes, osteoclasts, and vascular cells [33]. Osteogenesis of target gene-transduced BMSCs may exert its function via direct effects on BMSCs or by stimulating the formation of new blood vessels that invade the bone to

provide osteogenic cues and potentially deliver osteoblast progenitors via a cell nonautonomous mechanism [34]. It would be interesting to determine whether the ossification effect was also exerted in a paracrine manner or whether it was exerted solely directly through osteogenic differentiation of the BMSCs.

CONCLUSION

In conclusion, our results prove that in vitro genetic manipulation of BMSCs to overexpress *HIF-1 α* could greatly improve osteogenesis and angiogenesis. Furthermore, the target gene-transduced BMSCs exhibit an increased ability to heal critical cranial defects in vivo. Impressively, cHIF showed significantly greater osteogenic and angiogenic activity in BMSCs compared with HIF, both in vitro and in vivo. This work may serve as evidence for further study of BMSCs engineered with *HIF-1 α* for bone regeneration. A prolonged observation in vivo must be considered to determine whether *HIF-1 α* is safe if we use *HIF-1 α* as a means of clinical treatment in the future.

ACKNOWLEDGMENTS

We thank Shanghai R&S Biotechnology Co., Ltd (China) for large-scale preparation of lentiviral vectors. This work was supported by the National Natural Science Foundation of China (81070806 and 81070864), NCET-08-0353, Science and Technology Commission of Shanghai Municipality (09411954800, 10JC1413300, 0952nm04000, 10430710900, and 10dz2211600), Science and Technology Commission of Anhui Municipality (11040606M173 and 11040606M204), and Key Project of Education Department of Anhui Province (KJ2009A037).

DISCLOSURE OF POTENTIAL CONFLICTS OF INTEREST

The authors indicate no potential conflicts of interest.

REFERENCES

- Bruder SP, Kurth AA, Shea M et al. Bone regeneration by implantation of purified, culture-expanded human mesenchymal stem cells. *J Orthop Res* 1998;16:155–162.
- Zhao Z, Wang Z, Ge C et al. Healing cranial defects with AdRunx2-transduced marrow stromal cells. *J Dent Res* 2007;86:1207–1211.
- Wang Y, Wan C, Deng L et al. The hypoxia-inducible factor alpha pathway couples angiogenesis to osteogenesis during skeletal development. *J Clin Invest* 2007;117:1616–1626.
- Wiesener MS, Turley H, Allen WE et al. Induction of endothelial PAS domain protein-1 by hypoxia: Characterization and comparison with hypoxia-inducible factor-1alpha. *Blood* 1998;92:2260–2268.
- Park SK, Dadak AM, Haase VH et al. Hypoxia-induced gene expression occurs solely through the action of hypoxia-inducible factor 1alpha (HIF-1alpha): Role of cytoplasmic trapping of HIF-2alpha. *Mol Cell Biol* 2003;23:4959–4971.
- Scortegagna M, Ding K, Oktay Y et al. Multiple organ pathology, metabolic abnormalities and impaired homeostasis of reactive oxygen species in *Epas1*-/- mice. *Nat Genet* 2003;35:331–340.
- Weidemann A, Johnson RS. Biology of HIF-1alpha. *Cell Death Differ* 2008;15:621–627.
- Sarkar K, Fox-Talbot K, Steenbergen C et al. Adenoviral transfer of HIF-1alpha enhances vascular responses to critical limb ischemia in diabetic mice. *Proc Natl Acad Sci USA* 2009;106:18769–18774.
- Mahon PC, Hirota K, Semenza GL. FIH-1: A novel protein that interacts with HIF-1alpha and VHL to mediate repression of HIF-1 transcriptional activity. *Genes Dev* 2001;15:2675–2686.
- Jaakkola P, Mole DR, Tian YM et al. Targeting of HIF-1alpha to the von Hippel-Lindau ubiquitylation complex by O2-regulated prolyl hydroxylation. *Science* 2001;292:468–472.
- Bruder SP, Fox BS. Tissue engineering of bone. Cell based strategies. *Clin Orthop Relat Res* 1999;S68–S83.
- Liechty KW, MacKenzie TC, Shaaban AF et al. Human mesenchymal stem cells engraft and demonstrate site-specific differentiation after in utero transplantation in sheep. *Nat Med* 2000;6:1282–1286.
- Tsuda H, Wada T, Ito Y et al. Efficient BMP2 gene transfer and bone formation of mesenchymal stem cells by a fiber-mutant adenoviral vector. *Mol Ther* 2003;7:354–365.
- Zhang C, Wang KZ, Qiang H et al. Angiopoiesis and bone regeneration via co-expression of the hVEGF and hBMP genes from an adeno-associated viral vector in vitro and in vivo. *Acta Pharmacol Sin* 2010;31:821–830.
- Maniopoulos C, Sodek J, Melcher AH. Bone formation in vitro by stromal cells obtained from bone marrow of young adult rats. *Cell Tissue Res* 1988;254:317–330.

- 16 Li Y, Liu X, Liu C et al. Improvement of morphine-mediated analgesia by inhibition of beta-arrestin 2 expression in mice periaqueductal gray matter. *Int J Mol Sci* 2009;3:954–63.
- 17 Jing Q, Xin SM, Cheng ZJ et al. Activation of p38 mitogen-activated protein kinase by oxidized LDL in vascular smooth muscle cells: Mediation via pertussis toxin-sensitive G proteins and association with oxidized LDL-induced cytotoxicity. *Circ Res* 1999;84:831–839.
- 18 Kasten P, Luginbuhl R, van GM, et al. Comparison of human bone marrow stromal cells seeded on calcium-deficient hydroxyapatite, beta-tricalcium phosphate and demineralized bone matrix. *Biomaterials* 2003;24:2593–2603.
- 19 Livak KJ, Schmittgen TD. Analysis of relative gene expression data using real-time quantitative PCR and the 2⁻($\Delta\Delta C_T$) Method. *Methods* 2001;25:402–408.
- 20 Koh JT, Zhao Z, Wang Z et al. Combinatorial gene therapy with BMP2/7 enhances cranial bone regeneration. *J Dent Res* 2008;87:845–849.
- 21 Mardas N, Stavropoulos A, Karring T. Calvarial bone regeneration by a combination of natural anorganic bovine-derived hydroxyapatite matrix coupled with a synthetic cell-binding peptide (PepGen): An experimental study in rats. *Clin Oral Implants Res* 2008;19:1010–1015.
- 22 Bolland BJ, Kanczler JM, Dunlop DG et al. Development of in vivo μ CT evaluation of neovascularisation in tissue engineered bone constructs. *Bone* 2008;43:195–202.
- 23 Cacciafesta V, Dalstra M, Bosch C et al. Growth hormone treatment promotes guided bone regeneration in rat calvarial defects. *Eur J Orthod* 2001;23:733–740.
- 24 Sun XJ, Zhang ZY, Wang SY et al. Maxillary sinus floor elevation using a tissue-engineered bone complex with OsteoBone and bMSCs in rabbits. *Clin Oral Implants Res* 2008;19:804–813.
- 25 Majmundar AJ, Wong WJ, Simon MC. Hypoxia-inducible factors and the response to hypoxic stress. *Mol Cell* 2010;40:294–309.
- 26 Kelly BD, Hackett SF, Hirota K et al. Cell type-specific regulation of angiogenic growth factor gene expression and induction of angiogenesis in nonischemic tissue by a constitutively active form of hypoxia-inducible factor 1. *Circ Res* 2003;93:1074–1081.
- 27 Manalo DJ, Rowan A, Lavoie T et al. Transcriptional regulation of vascular endothelial cell responses to hypoxia by HIF-1. *Blood* 2005;105:659–669.
- 28 Jiang X, Gittens SA, Chang Q et al. The use of tissue-engineered bone with human bone morphogenetic protein-4-modified bone-marrow stromal cells in repairing mandibular defects in rabbits. *Int J Oral Maxillofac Surg* 2006;35:1133–1139.
- 29 Riley EH, Lane JM, Urist MR et al. Bone morphogenetic protein-2: Biology and applications. *Clin Orthop Relat Res* 1996;324:39–46.
- 30 Grayson WL, Zhao F, Izadpanah R et al. Effects of hypoxia on human mesenchymal stem cell expansion and plasticity in 3D constructs. *J Cell Physiol* 2006;207:331–339.
- 31 Rohanizadeh R, Swain MV, Mason RS. Gelatin sponges (Gelfoam) as a scaffold for osteoblasts. *J Mater Sci Mater Med* 2008;19:1173–1182.
- 32 Rey S, Lee K, Wang CJ et al. Synergistic effect of HIF-1 α gene therapy and HIF-1-activated bone marrow-derived angiogenic cells in a mouse model of limb ischemia. *Proc Natl Acad Sci USA* 2009;106:20399–20404.
- 33 Wan C, Shao J, Gilbert SR et al. Role of HIF-1 α in skeletal development. *Ann N Y Acad Sci* 2010;1192:322–326.
- 34 Liu L, Marti GP, Wei X et al. Age-dependent impairment of HIF-1 α expression in diabetic mice: Correction with electroporation-facilitated gene therapy increases wound healing, angiogenesis, and circulating angiogenic cells. *J Cell Physiol* 2008;217:319–327.



See www.StemCells.com for supporting information available online.